Simulating incoherent multicomponent nonstationary ground motions conditioned on observed records

X.Z. Cui[1] and H.P. Hong[2]

[1] Ph.D. Student, Department of Civil and Environment Engineering, University of Western Ontario – London, ON, Canada.

[2] Professor, Department of Civil and Environment Engineering, University of Western Ontario – London, ON, Canada.

ABSTRACT

Structures with multiple supports are subjected to spatially varying multicomponent seismic ground motions. Multicomponent seismic ground motions along different orientations and at spatially separated sites are incoherent. Such motions can be simulated using the spectral representation method for selected target evolutionary power spectral density functions, and coherency function. If a single or multiple ground motion records near a structure of interest are available, they can be used as the conditional ground motion records to simulation the motions at the supports of the considered structure. However, the existing procedure is computing time consuming, and could result in that the power spectral density function of the simulated ground motions differ from the target. These issues are explained and, a new procedure is proposed. An application of a newly proposed procedure that overcomes these drawbacks is illustrated.

Keywords: Earthquake, simulation, ground motions, multicomponent, nonstationary

INTRODUCTION

Linear and nonlinear time history analyses are often used to assess the response of structures and infrastructure systems subjected to seismic ground motions. Although the ground motions are spatially varying, for simplicity and due to lack of records that match the configuration of the foundation or multiple supports of a structural system, uniform excitation is often considered for structures with multiple supports. This is partly due to unavailability of the historical records that match the layout of the supports of multi-support structures. The consideration of spatially varying ground motions for structures with multiple support and irregular shapes are discussed in many studies ([1-3] and references thereafter). To overcome the lack of adequate historical records, the spatially varying ground motions at multiple supports may be obtained through numerical simulation.

The simulation can be carried out using the spectral representation method (SRM) [4-6] for given target power density function (PSD) or evolutionary power spectral density function (EPSD) [1,7] and coherency functions [8-11]. In addition, one could use the historical records as the conditional records to simulate spatially varying ground motion records [12-15]. The conditional simulation uses the properties of joint probability distribution of a set of normal variates conditioned on values of another set of normal variates. The conditional simulation is further investigated in [16,17]. These studies pointed out that the computation of the covariance matrix of the Fourier coefficients used to represent the ground motion time histories can be evaluated based on the fast Fourier transform (FFT) algorithm to reduce computing time.

In all case, application of the existing algorithm may not converge due to the difficulty in inverting (conditioning) covariance matrix of the Fourier coefficients. In the present study, we provide a new practical procedure by modifying the commonly used Fourier series representation of the nonstationary ground motions, using the PSD from the conditioning ground motions and truncating the first few terms in the series representation of the ground motions. It is shown through a numerical example that the proposed modification overcomes the observed drawbacks. The procedure is illustrated through a numerical example.

CONDITIONAL SIMULATION OF NONSTATIONARY PROCESS

Evolutionary spectral representation and conditional simulation

Consider a vector of nonstationary process $\boldsymbol{X}(t)$ with component $X_j(t)$, $j = 1, \ldots, n$, where $X_j(t)$ is a zero-mean nonstationary stochastic process admitting the evolutionary spectral representation [18],

$$X_j(t) = \int_{-\infty}^{+\infty} a_j(\omega, t) \exp(i\omega t) dZ_j(\omega) \tag{1}$$

$X_j(t) = \int_{-\infty}^{+\infty} a_j(\omega, t) \exp(i\omega t) dZ_j(\omega)$ where $i = \sqrt{-1}$; ω is frequency, $a_j(\omega, t)$ is a slowly varying function of time t for given ω; $Z_j(t)$ and $Z_k(t)$ are zero-mean stationary Gaussian processes with orthogonal increment, and (double-sided) PSD and crossed PSD functions denoted by $S_{jk}(\omega)$, where

$$S_{jk}(\omega) = \sqrt{S_{jj}(\omega) S_{kk}(\omega)} \times \gamma_{jk}(\omega) \tag{2}$$

and $\gamma_{jk}(\omega)$ is the coherency function. The evolutionary PSD (EPSD) and crossed EPSD functions of $X_j(t)$ and $X_k(t)$ are given by,

$$S_{jk}(\omega, t) = \left(a_j(\omega, t)\right)\left(a_k(\omega, t)\right)^* \sqrt{S_{jj}(\omega) S_{kk}(\omega)} \times \gamma_{jk}(\omega) \tag{3}$$

where $S_{jj}(\omega,t)$ denotes the EPSD function and $S_{jk}(\omega,t)$ denotes the crossed EPSD function, the superscript * denote the complex conjugate. The $n\times n$ EPSD matrix of $\boldsymbol{X}(t)$, $\boldsymbol{S}(\omega,t)$, is defined with elements $S_{jk}(\omega,t)$. The assessment of the EPSD was studied by several researchers [19,20]; the investigation of the coherency was given in [2,8-11,21].

Based on SRM, $X_j(t)$ can be represented by [4],

$$X_j(t) = \frac{A_{j_1}}{2} + \sum_{p=2}^{N} \left(A_{jp} \cos \omega_p t + B_{jp} \sin \omega_p t \right) \tag{4}$$

where $\omega_p = (2\pi/T)\times(p-1)$, $N = 1+\omega_u/(2\pi/T)$, ω_u is the cut-off frequency, T is the duration, and A_{jp} and B_{jp} are the Fourier coefficients which are zero mean and jointly Gaussian random variables. The expectation of the product of the coefficients (i.e., second moments) can be evaluated and denoted as $E[A_{jp}A_{kq}]$, $E[A_{jp}B_{kq}]$, $E[B_{jp}A_{kq}]$ and $E[B_{jp}B_{kq}]$, where $j,k = 1,...,n$; $p,q = 1,...,N$ for A with subscripts; $p,q = 2,...,N$ for B with subscripts. The calculation of each of these expectations involves four-dimensional integral whose accurate evaluation is computing time consuming.

Let $\boldsymbol{F} = [\boldsymbol{F}_1^T, \boldsymbol{F}_2^T, ..., \boldsymbol{F}_n^T]^{\mathrm{T}}$ denote a vector of size $n(2N\text{-}1)$, where $\boldsymbol{F}_j = [A_{j1}, A_{j2}, ..., A_{jn}, B_{j2}, ..., B_{jn}]^{\mathrm{T}}$ is a $(2N\text{-}1)$ vector, and the superscript T denote the transpose. The covariance matrix of $\boldsymbol{F}$, $\boldsymbol{C_{FF}}$, is formed by $n\times n$ submatrices $\boldsymbol{C}_{\boldsymbol{F}_j\boldsymbol{F}_k}$, $j,k = 1,...,n$, where $\boldsymbol{C}_{\boldsymbol{F}_j\boldsymbol{F}_k}$ is a $(2N\text{-}1)\times(2N\text{-}1)$ matrix given by [14],

$$\boldsymbol{C}_{\boldsymbol{F}_j\boldsymbol{F}_k} = \begin{bmatrix} \boldsymbol{C}_{\boldsymbol{A}_j\boldsymbol{A}_k} & \boldsymbol{C}_{\boldsymbol{A}_j\boldsymbol{B}_k} \\ \boldsymbol{C}_{\boldsymbol{B}_j\boldsymbol{A}_k} & \boldsymbol{C}_{\boldsymbol{B}_j\boldsymbol{B}_k} \end{bmatrix}, \text{ with the sizes } \begin{bmatrix} N\times N & N\times(N-1) \\ (N-1)\times N & (N-1)\times(N-1) \end{bmatrix}, \; j,k = 1,...,n \tag{5}$$

in which the (p, q)-th element in $\boldsymbol{C}_{\boldsymbol{A}_j\boldsymbol{A}_k}$ is $E(A_{jp}A_{kq})$, in $\boldsymbol{C}_{\boldsymbol{A}_j\boldsymbol{B}_k}$ is $E(A_{jp}B_{kq})$, in $\boldsymbol{C}_{\boldsymbol{B}_j\boldsymbol{A}_k}$ is $E(B_{jp}A_{kq})$, and in $\boldsymbol{C}_{\boldsymbol{B}_j\boldsymbol{B}_k}$ is $E(B_{jp}B_{kq})$; $E(\;)$ denotes the expectation; $p,q = 1,...,N$ for A with subscripts; and $p,q = 2,...,N$ for B with subscripts.

Since the coefficients A_{jp} and B_{kq} are zero-mean jointly Gaussian random variables, and the elements in $\boldsymbol{C_{FF}}$ can be evaluated based on $S_{jk}(\omega,t)$, samples of A_{jp} and B_{kq} can be simulated from the joint normal distribution and Eq. (4) can be used to obtain synthetic seismic ground motions.

If some elements in $\boldsymbol{X}(t)$, that are included in $(\boldsymbol{X}_o(t))$ is observed and the simulation of remaining unobserved elements in $\boldsymbol{X}(t)$, that are included in $(\boldsymbol{X}_u(t))$, conditioned on $(\boldsymbol{X}_o(t))$ is of interest, where $\boldsymbol{X}_o(t)$ and $\boldsymbol{X}_u(t)$ are vectors of size n_o and $(n\text{-}n_o)$, respectively. Accordingly, $\boldsymbol{F}$ is partitioned into $[\boldsymbol{F}_o^{\mathrm{T}}, \boldsymbol{F}_u^{\mathrm{T}}]^{\mathrm{T}}$, representing the vectors of size $n_o(2N\text{-}1)$ and $(n\text{-}\ n_o)(2N\text{-}1)$, respectively. $\boldsymbol{C_{FF}}$ is then partitioned according to $\boldsymbol{F}_o$ and $\boldsymbol{F}_u$ as,

$$\boldsymbol{C}_{FF} = \begin{bmatrix} \boldsymbol{C}_{Foo} & \boldsymbol{C}_{Fou} \\ \boldsymbol{C}_{Fuo} & \boldsymbol{C}_{Fuu} \end{bmatrix}, \text{ with the sizes } \begin{bmatrix} \left(n_o(2N-1)\right)\times\left(n_o(2N-1)\right) & \left(n_o(2N-1)\right)\times\left((n-n_o)(2N-1)\right) \\ \left((n-n_o)(2N-1)\right)\times\left(n_o(2N-1)\right) & \left((n-n_o)(2N-1)\right)\times\left((n-n_o)(2N-1)\right) \end{bmatrix} \tag{6}$$

where $\boldsymbol{C}_{\tilde{F}oo} = E(\tilde{\boldsymbol{F}}_o\tilde{\boldsymbol{F}}_o^T)$, $\boldsymbol{C}_{\tilde{F}ou} = E(\tilde{\boldsymbol{F}}_o\tilde{\boldsymbol{F}}_u^T)$, $\boldsymbol{C}_{\tilde{F}uo} = E(\tilde{\boldsymbol{F}}_u\tilde{\boldsymbol{F}}_o^T)$ and $\boldsymbol{C}_{\tilde{F}uu} = E(\tilde{\boldsymbol{F}}_u\tilde{\boldsymbol{F}}_u^T)$.

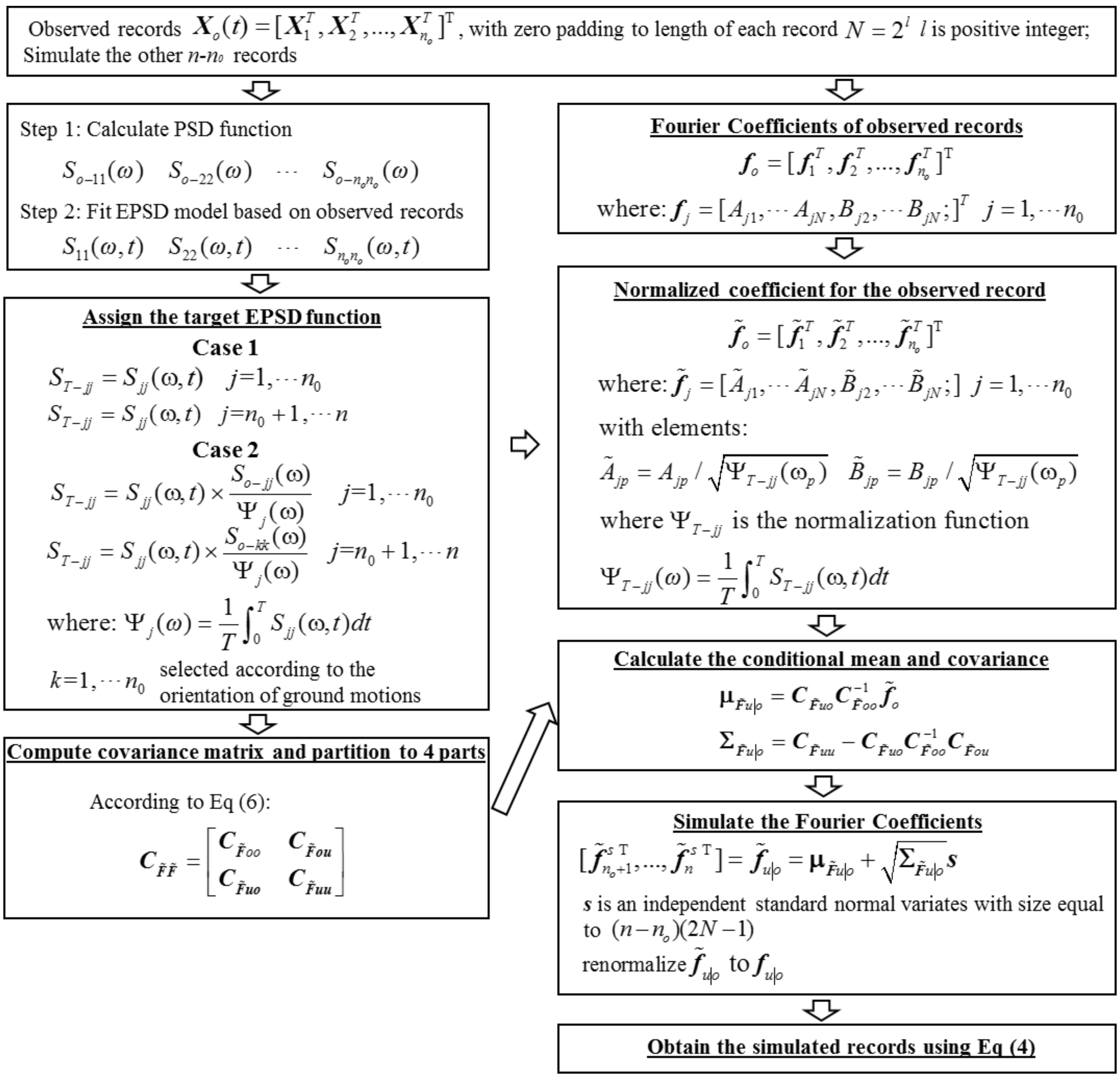

Figure 1. Flow chart of conditional simulation procedure (details and interpretations can be found in [22])

The value of $\boldsymbol{F}_o$, $\boldsymbol{f}_o = [\boldsymbol{f}_1^T, \boldsymbol{f}_2^T, ..., \boldsymbol{f}_{n_o}^T]^{\mathrm{T}}$, is calculated considering that $\boldsymbol{X}_o(t)$ can be represented using Eq. (3) (where the definition of $\boldsymbol{F}_o$ is similar to $\boldsymbol{F}$ discussed in the previous paragraph). Based on the properties of zero-mean multivariate normal variates, the variables in $\boldsymbol{F}_u$ conditioned on $\boldsymbol{F}_o = \boldsymbol{f}_o$, $\boldsymbol{F}_{u|o}$, are also jointly Gaussian random variables with the mean and the covariance matrix, denoted by $\boldsymbol{\mu}_{\boldsymbol{F}u|o}$ and $\boldsymbol{\Sigma}_{\boldsymbol{F}u|o}$, where,

$$\boldsymbol{\mu}_{\boldsymbol{F}u|o} = \boldsymbol{C}_{\boldsymbol{F}uo}\boldsymbol{C}_{\boldsymbol{F}oo}^{-1}\boldsymbol{f}_o \tag{7}$$

and,

$$\boldsymbol{\Sigma}_{\boldsymbol{F}u|o} = \boldsymbol{C}_{\boldsymbol{F}uu} - \boldsymbol{C}_{\boldsymbol{F}uo}\boldsymbol{C}_{\boldsymbol{F}oo}^{-1}\boldsymbol{C}_{\boldsymbol{F}ou} \tag{8}$$

They can be used to simulate the coefficients A and B (with subscripts) in $\boldsymbol{F}_u$, so the conditionally simulated ground motions $\boldsymbol{X}_u(t)$ can be calculated by using Eq. (4).

Our experience indicates that non-convergence problem frequently occurs when calculating the inverse matrix of $\boldsymbol{C}_{\boldsymbol{F}oo}$. Also, the PSD or EPSD of the simulated ground motions deviates from the assigned target PSD which is based fitted EPSD function. The cause of non-convergence is partly due to the significant changes in the diagonal elements of $\boldsymbol{C}_{\boldsymbol{F}oo}$, which is attributed to the variation of the EPSD function in frequency. The deviation to the original target can be explained but may not be suitable for engineering application considering that the PSD of a ground motion record is associated with event-to-event variation.

A modified conditional simulation procedure to avoid the non-convergence in inverting the matrix is proposed and illustrated in the flow chart shown in Figure 1. The modification consists of introducing a new normalization functions $\psi_{T\text{-}jj}(\omega)$ and providing an approach to assign the target EPSD. The latter reduces potential bias in the EPSD of the simulated records, and the former can reduce the condition number of $\boldsymbol{C}_{\boldsymbol{F}oo}$, so to possibly eliminate the non-convergence problem in inverting $\boldsymbol{C}_{\boldsymbol{F}oo}$. Additional effort in reducing the condition number of the matrix is to eliminate first few terms in Eq. (4); the elimination of these terms with very low frequencies do not affect their engineering applications.

Case-2 shown in Figure 1 emphasizes the event-to-event variability of PSD function, while Case-1 emphasizes that the PSD function at considered site for all events are homogeneous.

NUMERICAL EXAMPLES

In this section, conditionally simulated bidirectional ground motions are presented. The layout of the sites is as shown in Figure 2a. The observed two horizontal orthogonal record components at Bear Valley #12, Williams Ranch for the Loma Prieta earthquake is considered as the conditioning ground motions at Site 1. The record components extracted from http://peer.berkeley.edu/nga/index.html are shown in Figure 2b for Site 1.

For the numerical analysis, it is considered that the auto-EPSD function can be expressed as,

$$S_{jj}(\omega,t) = \frac{\left(C_0\sigma_a(t)\right)^2 \times \left[1+4\xi_g^2(\omega/\omega_g(t))^2\right]}{[1-(\omega/\omega_g(t))^2]^2 + 4\xi_g^2(\omega/\omega_g(t))^2} \times \frac{\omega^4}{(\omega^2-\omega_f(t)^2)^2 + 4\omega^2\omega_f(t)^2\xi_f^2} \tag{9}$$

where C_0 is a constant; $\sigma_a(t)$ is a time varying amplitude; ξ_g is the effective ground damping that depends on the soil type; ξ_f is a filter damping; $\omega_f(t)$ equals $c_\omega\omega_g(t)$ in which c_ω is a constant to ensure the consistency of power of ground motions; $\omega_g(t) = \pi F_c(t)$ in which $F_c(t) = F_0 + F_1(e^{-b_1 t} - e^{-b_2 t})$ is the zero-crossing rate and F_0, F_1, b_1 and b_2 are model coefficients [23]. The parameters for the model shown in Eq. (9) estimated by following the procedure similar to [20,23] are shown in Table 1. The ground motions at Sites 2 to 6 conditioned on the observed record components at Site 1 are to be simulated. For the simulation, the wave is considered to travel in the direction from Site 1 to Site 6 with v_{app} equal to 2000 m/s. It is considered that the lagged coherency for the horizontal ground motion components oriented along the same direction, $\left|\overline{\gamma}_{HH}(d,f)\right|$, given below is applicable [9,21],

$$\left|\overline{\gamma}_{HH}(d,f)\right| = A\exp\left(-\frac{2d}{\alpha_0\theta(f)}\left(1-A+\alpha_0 A\right)\right) + \left(1-A\right)\exp\left(-\frac{2d}{\theta(f)}\left(1-A+\alpha_0 A\right)\right) \tag{10}$$

where d (m) is the distance between two sites; f is frequency in Hz; $\theta(f) = k\left(1+(f/f_0)^B\right)^{-1/2}$, A = 0.5, α_0 = 1.60×10^{-4}, k = 3.00×10^7, f_0 =2.5 and B =5.7.

The lagged coherency for the record components oriented along the same direction but at different sites are defined by Eq. (11), and that for the horizontal orthogonal components, $|\gamma_{_{HO}}(d, f)|$, is given by,

$$|\gamma_{_{HO}}(d, f)| = c_0 - c_1 f \tag{11}$$

where $c_0 = 0.52$ and $c_1 = 2.70\times10^{-3}$ [21].

The results shown in Figure 2b for Site 2 to 6 by assigning the target PSD function according to Case-1. Figure 3c indicates that as the site moves away from the site of conditional record, the PSD function of the simulated record matches target PSD function.

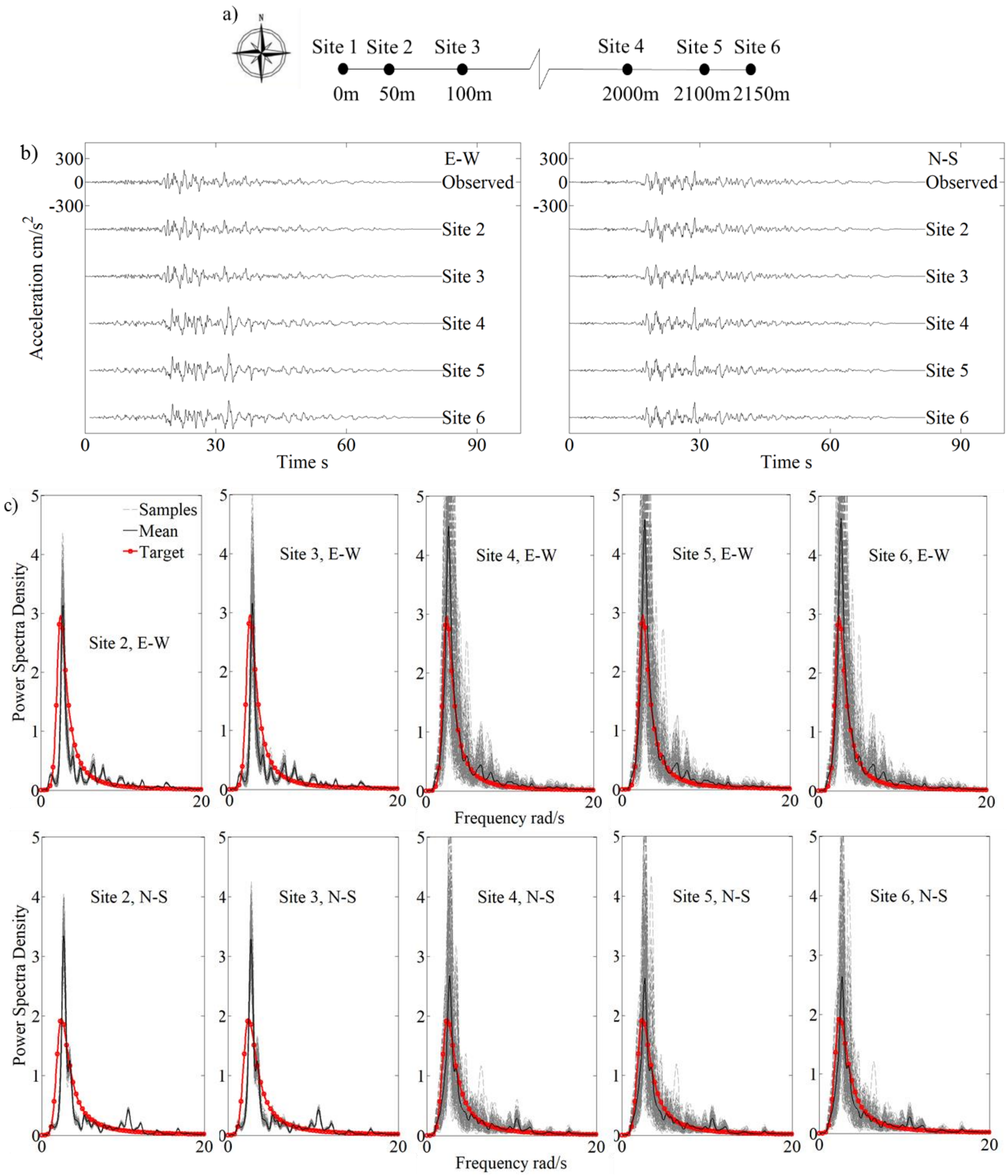

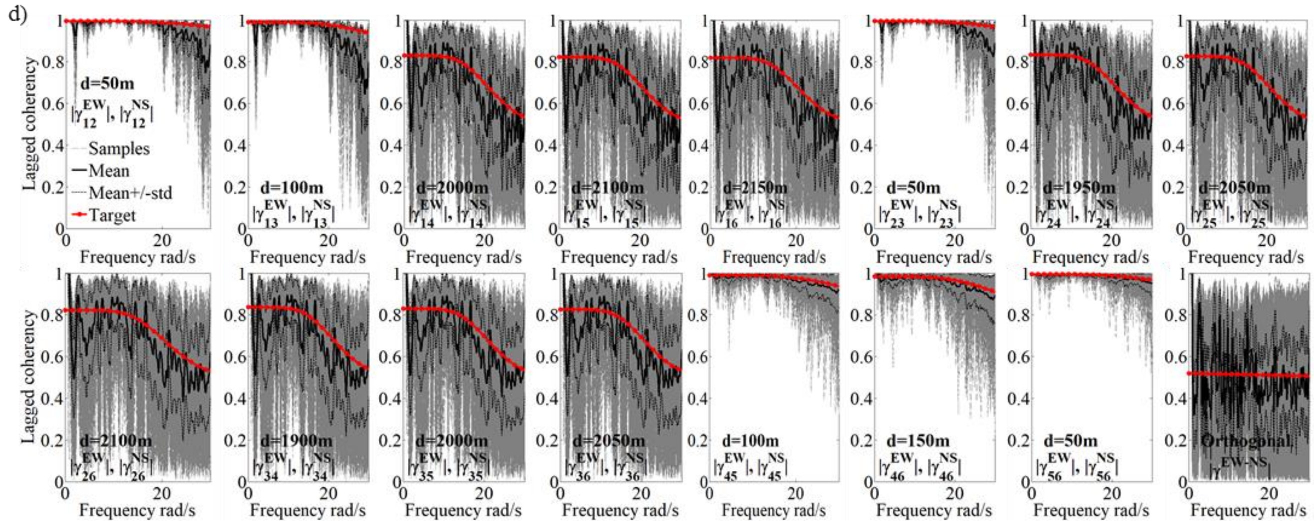

Figure 2: Layouts of sites for the conditional simulation of bidirectional horizontal ground motions by considering Case-1, and estimated PSD functions and lagged coherencies: a) A set of samples of ground motions; b) Computed PSD density function (cm^2/(s^{3}rad)) from simulated ground motions; c) Computed lagged coherency from simulated ground motions ($|\gamma_{jk}|$) denotes the lagged coherency between site j and k, additional subscripts denotes the orientation of ground motions; ($|\gamma^{EWNS}|$) denotes the lagged coherencies in two orthogonal horizontal directions).

Table 1: Model parameters of EPSD functions for three observed record components.

Model parameters	Loma Prieta E-W	Loma Prieta N-S
ξ_g	0.60	0.6
ξ_f	0.30	0.48
C_0	0.82	0.90
F_0(1/s)	0.87	0.75
F_1(1/s)	5.41	3.73
b_1(1/s)	0.33	0.30
b_2(1/s)	0.60	0.71
c_ω	0.82	0.90
T (s)	78.25	78.25

Rather than considering Case-1, Case-2 is considered and the analyses carried out for the results shown in Figure 2 are repeated. The obtained results are shown in Figure 3, indicating that the adequacy of PSD of simulated records.

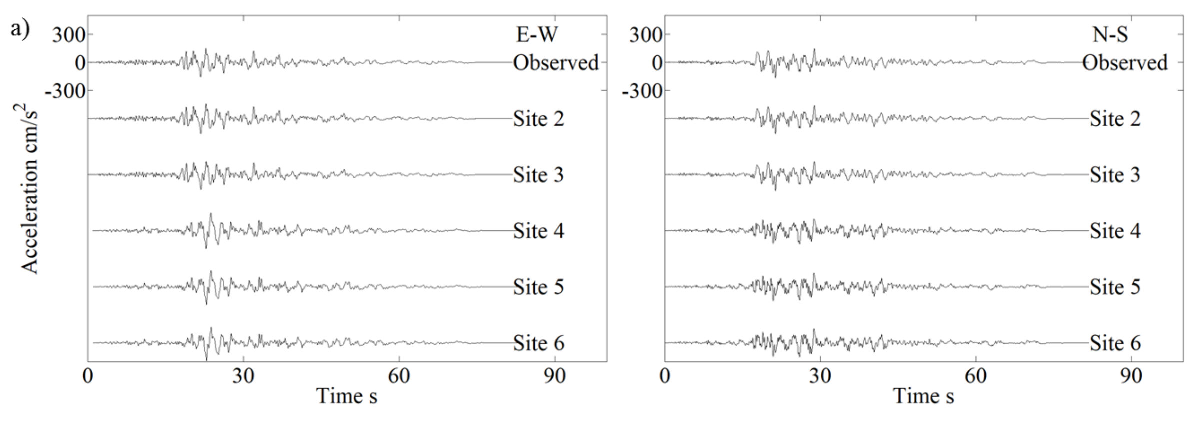

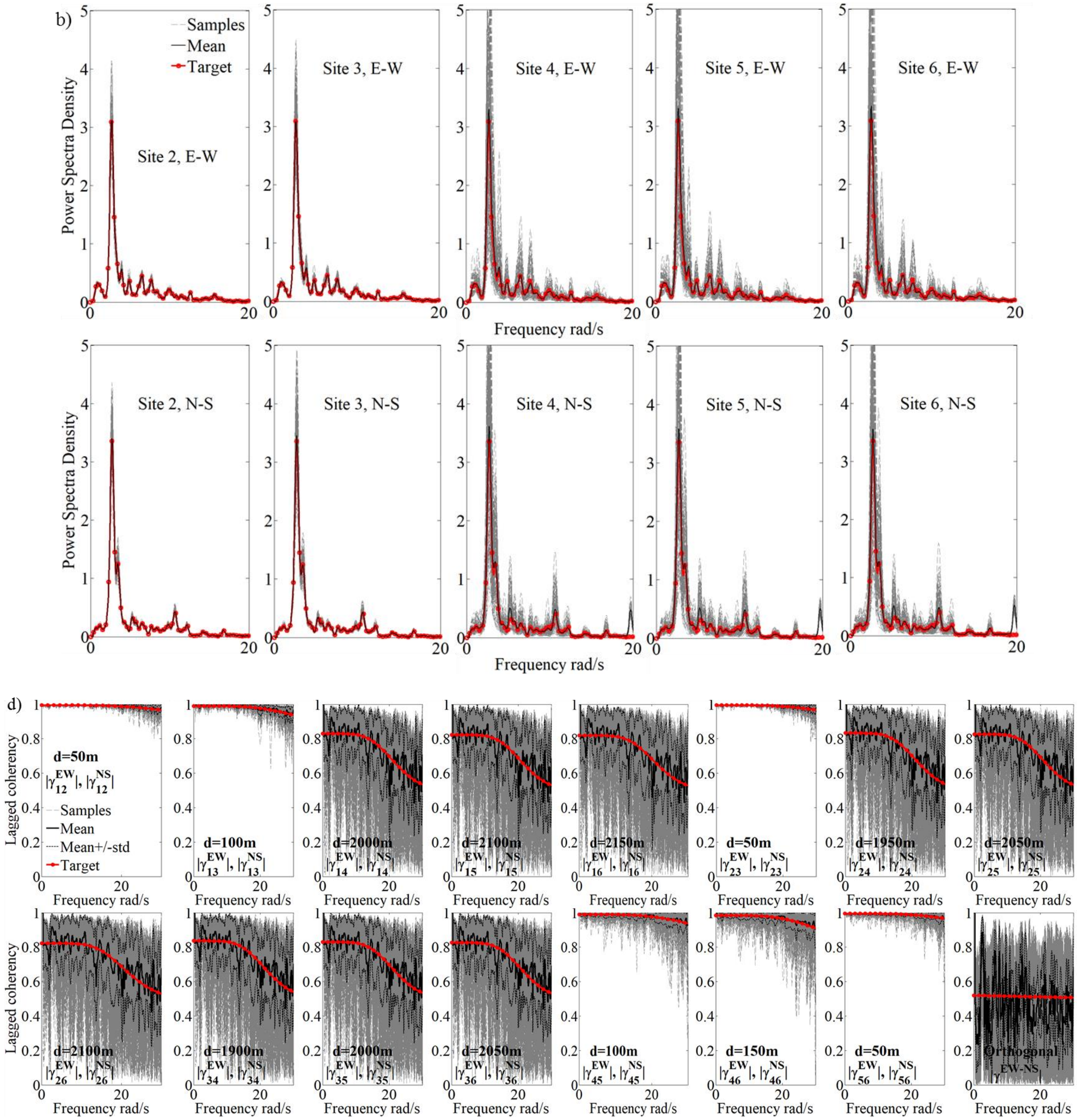

Figure 3. Conditional simulation by considering Case-2, and statistics of the PSD function and lagged coherency: a) A set of samples of conditionally simulated ground motions; b) Computed PSD function (cm^2/(s^{3}rad)) from simulated ground motions; and c) Computed lagged coherency from simulated ground motions ($|\gamma_{jk}|$ denotes the lagged coherency between site j and k).

CONCLUSIONS

A modified conditional simulation procedure is proposed to avoid the non-convergence problem to invert the covariance matrix (hence, the breakdown of conditional simulation procedure), and to better match the target PSD function. Two interpretations to assign the target PSD function discussed. The results show that in Case-1, the PSD functions of simulated records match the observed PSD functions for sites near the conditional records and matches the targets for sites away from the observation sites. This is consistent with Bayesian updating procedure. By considering event-to-event variability in assigning the target PSD function, in Case-2, the PSD functions of the simulated records consistently match those of targets.

ACKNOWLEDGMENTS

Financial support received from the National Science and Engineering Research Council of Canada (RGPIN-2016-04814 for HPH, CREAT-482707-2016), the University of Western Ontario and the China Scholarship Council (No.201707980007 for XC) is gratefully acknowledged.

REFERENCES

[1] Clough, R. W., and Penzien, J. (2003). Dynamics of structures. USA: Computers and Structures.
[2] Zerva, A. (2009). Spatial variation of seismic ground motion. Modeling and engineering applications. CRC Press, Taylor & Francis Group, Boca Raton, FL.
[3] Liu, T.J. and Hong, H.P. (2013) Simulation of multiple-station ground motions using stochastic point-source method with spatial coherency and correlation characteristics, Bulletin of the Seismological Society of America, 103(3), 1912–1921.
[4] Shinozuka, M. and Jan, C. M. (1972). Digital simulation of random processes and its applications. Journal of Sound and Vibration, 25(1), 111-128.
[5] Grigoriu, M. (1993). Simulation of nonstationary gaussian processes by random trigonometric polynomials. Journal of Engineering Mechanics, ASCE, 119(2), 328-343.
[6] Shinozuka, M. and Deodatis, G. (1996). Simulation of multi-dimensional Gaussian stochastic fields by spectral representation. Applied Mechanics Reviews, 49(1), 29-53.
[7] Boore, D. M. (2009). Comparing stochastic point-source and finite-source ground-motion simulations: SMSIM and EXSIM. Bulletin of the Seismological Society of America, 99(6), 3202-3216.
[8] Harichandran, R. S., and Vanmarcke, E. H. (1986). Stochastic variation of earthquake ground motion in space and time. Journal of Engineering Mechanics, ASCE, 112(2), 154-174.
[9] Hao, H., Oliveira, C. S., and Penzien, J. (1989). Multiple-station ground motion processing and simulation based on SMART-1 array data. Nuclear Engineering and Design, 111(3), 293-310.
[10] Der Kiureghian, A. D. (1996). A coherency model for spatially varying ground motions. Earthquake Engineering and Structural Dynamics, 25(1), 99-111.
[11] Hong, H. P., and Liu, T. J. (2014). Assessment of coherency for bidirectional horizontal ground motions and its application for simulating records at multiple stations. Bulletin of the Seismological Society of America, 104(5), 2491-2502.
[12] Kameda, H., and Morikawa, H. (1994). Conditioned stochastic processes for conditional random fields. Journal of Engineering Mechanics, ASCE, 120(4), 855-875.
[13] Vanmarcke, E. H., and Fenton, G. A. (1991). Conditioned simulation of local fields of earthquake ground motion. Structural Safety, 10(1-3), 247-264.
[14] Vanmarcke, E. H., Heredia-Zavoni, E., and Fenton, G. A. (1993). Conditional simulation of spatially correlated earthquake ground motion. Journal of Engineering Mechanics, ASCE, 119(11), 2333-2352.
[15] Shinozuka, M. and Zhang, R. (1996). Equivalence between Kriging and CPDF methods for conditional simulation. Journal of Engineering Mechanics, ASCE, 122(6), 530-538.
[16] Hu, L., Xu, Y. L., and Zheng, Y. (2012). Conditional simulation of spatially variable seismic ground motions based on evolutionary spectra. Earthquake Engineering and Structural Dynamics, 41(15), 2125-2139.
[17] Xu, Y. L., Hu, L., and Kareem, A. (2012). Conditional simulation of nonstationary fluctuating wind speeds for long-span bridges. Journal of Engineering Mechanics, ASCE, 140(1), 61-73.
[18] Priestly, M. B. (1988). The Spectral Analysis of Time Series. New York: Academic Press.
[19] Yeh, C. H., and Wen, Y. K. (1990). Modeling of nonstationary ground motion and analysis of inelastic structural response. Structural Safety, 8(1-4), 281-298.
[20] Fan, F. G., and Ahmadi, G. (1990). Nonstationary Kanai-Tajimi models for el Centro 1940 and Mexico City 1985 earthquakes. Probabilistic Engineering Mechanics, 5(4), 171-181.
[21] Liu, T. J., and Hong, H. P. (2016). Assessment of spatial coherency using tri-directional ground motions. Journal of Earthquake Engineering, 20(5), 773-794.
[22] Cui, X.Z., and Hong, H. P. (2018). Conditional Simulation of Spatially Varying Multicomponent Nonstationary Ground Motions – Bias and Ill-condition (Submitted).
[23] Ellis, G. W., Cakmak, A. S., and Ledolter, J. (1987). Modelling earthquake ground motions in seismically active regions using parametric time series methods. In Developments in Geotechnical Engineering (Vol. 44, pp. 551-566). Elsevier, Amsterdam.